

Indirectly Manipulating Nanoscale Localized Fields of Bowtie Nanoantennas with Asymmetric Nanoapertures

Jianxiong Li · Shuqi Chen · Ping Yu · Hua Cheng · Lunjie Chen · Jianguo Tian

Received: 23 June 2012 / Accepted: 6 August 2012 / Published online: 19 August 2012
© Springer Science+Business Media, LLC 2012

Abstract We present a novel composite nanostructure consisting of bowtie nanoantennas and asymmetric nanoapertures, which provides a new way of indirectly tuning the resonant wavelengths and manipulating the localized fields. The proposed composite nanostructure cannot only produce a symmetric localized field distribution but also create two asymmetric localized field distributions in optical frequency. The resonant peaks of the composite nanostructure can easily be bidirectionally tuned by indirectly adjusting the geometrical parameters of the asymmetric nanoapertures. The mechanisms for manipulating and tuning the localized fields are also discussed.

Keywords Asymmetric nanoapertures · Bowtie nanoantennas · Asymmetric localized field · Indirectly manipulating

Introduction

Bowtie nanoantennas (BNAs), a typical structure of metamaterials, can convert freely propagating optical radiation into localized energy and generate large enhancement and confinement of light within deep sub-wavelength volumes by the plasmonic resonance and

curvature effect of bowtie tips [1–4]. A central goal of BNAs is to provide an enabling technology for complete manipulation and control over optical radiation at deep subwavelength scales. This manipulation capability is mainly reflected in two aspects, namely spectral steering of the resonant wavelength and spatial manipulation of the optical field distribution, which can contribute to a wide range of applications in nanolithography [5, 6], fluorescence enhancement [7, 8], and surface-enhanced Raman scattering (SERS) [9, 10]. Steering the resonant wavelength of BNAs can be realized by adjusting the nanogap between the BNAs [11]. However, increasing the nanogap may induce negative effects on the coupling between the two triangles of the BNAs, which will result in a reduction in the level of the localized field enhancement. Recently, Yang et al. proposed an asymmetric BNA that introduced a sharp angle for one triangle [12]. The resonant wavelength can be tuned by changing the degree of sharpness of one of the triangles, whereas the BNAs with sharp angles have reached the current fabrication limits. Zhang et al. also presented a class of asymmetric double BNAs oriented in a cross geometry [13]. The spectral properties and localized spatial mode distributions can be readily tuned by shifting the vertical BNA in the horizontal direction. However, a symmetric localized field distribution cannot be obtained from the asymmetric double BNAs, and the localized field enhancement generated by this configuration is still very low, which limits the applications of the BNAs in areas such as SERS and optical sorting or tapping. Moreover, the works in Refs. [11–13] mainly focus on directly adjusting the dimensions of the BNAs to manipulate optical radiation at the nanoscale, which constrains the mechanisms for steering optical field distributions.

J. Li · S. Chen (✉) · P. Yu · H. Cheng · L. Chen · J. Tian (✉)
The Key Laboratory of Weak Light Nonlinear Photonics,
Ministry of Education, School of Physics and TEDA
Applied Physics School, Nankai University,
Tianjin 300457, China
e-mail: schen@nankai.edu.cn
e-mail: jjtian@nankai.edu.cn

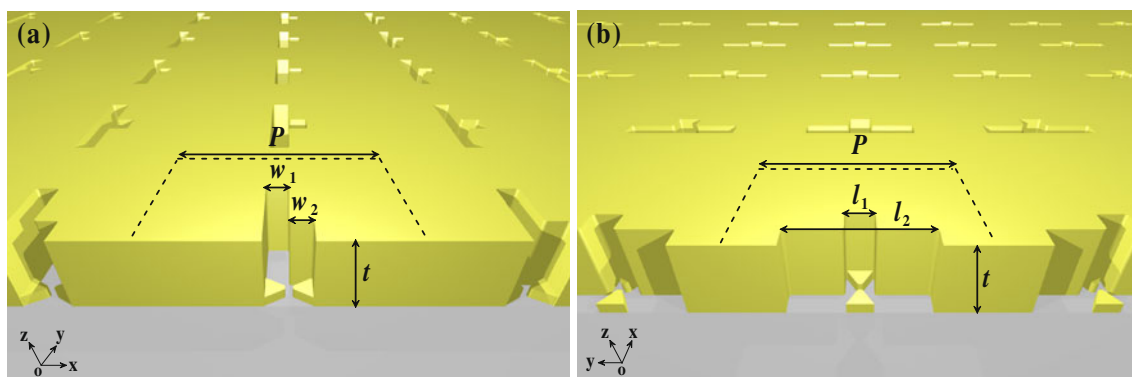


Fig. 1 Schematic illustrations of the CBA. **a** In the x - z plane cross sections, $w_1 = 50$ nm and $w_2 = 50$ nm. **b** In the y - z plane cross sections, $l_1 = 80$ nm and $l_2 = 240$ nm. In both, $P = 400$ nm and $t = 100$ nm

In this paper, we propose a periodic composite nanostructure consisting of BNAs and asymmetric nanoapertures (ANAs), which we refer to as the combination of BNAs and ANAs (CBAs) and which provides a new way of indirectly tuning the resonant wavelengths and manipulating the localized fields. The presented CBAs exhibit two distinct resonant peaks, which correspond to two asymmetric modes. The resonant peaks of the CBAs can easily be bidirectionally tuned by indirectly adjusting the geometrical parameters of the ANAs while preserving the large localized field enhancement and confinement. When the wavelength of incident light is far away from the resonant peaks, the distributions of the E-fields are symmetrical in the gap region of the BNAs. The mechanisms for manipulating and tuning the localized fields are also discussed.

Combination of BNAs and ANAs

The geometry of the proposed CBA is shown in Fig. 1. The Au layer with ANA is placed on the glass layer in the unit cell. A 20-nm-thick BNA is located at the bottom of the ANA. The symmetry axis of the BNA parallel to the perpendicular bisector of the triangle is overlapped with that of the ANA. Each constituent Au equilateral triangle of the bowtie has a perpendicular bisector length of 40 nm with a radius of curvature of 6.3 nm in the corner. The permittivity of gold is described by the Drude model with the relative permittivity at infinite frequency $\epsilon_\infty = 9.0$, the plasma frequency $\omega_p = 1.3166 \times 10^{16} \text{ s}^{-1}$, and the damping constant $\gamma = 1.3464 \times 10^{14} \text{ s}^{-1}$ [14]. The permittivity of the glass substrate is taken to be 2.25. The numerical calculations are carried out by the finite element method using COMSOL Multiphysics [15]. The CBA is illuminated by normally incident light, linearly polarized along the x direction. At the top and bottom of the simulation

domain, perfectly matched layers are placed in the z direction to completely absorb the waves leaving the simulation domain in the direction of propagation. Periodic boundary conditions are used in the x and y directions. The near-field intensity spectra are plotted by the maximum normalized e-field intensity within the plane through the center of the BNA in the z direction at each wavelength.

The Optical Properties of CBAs

A number of recent publications have discussed the optical properties of solitary BNAs, which exhibit a single resonant peak and localized field enhancement (as shown in Fig. 2). However, the proposed CBAs have two distinct resonant peaks at 700 and 780 nm (as also shown in Fig. 2). The two resonant peaks of CBAs correspond to the two waveguide modes of two rectangular nanoapertures with different sizes [16]. As the external E-field of the BNAs at the bottom of

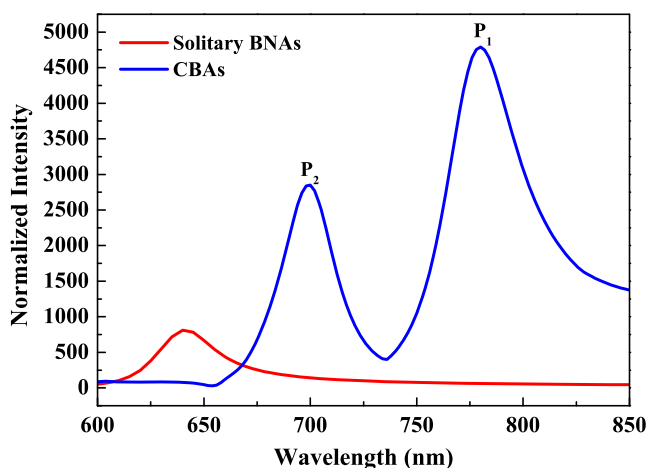


Fig. 2 Calculated normalized intensity spectra for solitary BNAs and CBAs

the ANAs is completely affected as determined by the waveguide modes of the ANAs, the intrinsic resonance of the BNAs in the CBAs is weak and indistinct in Fig. 2. Thus, dual resonant peaks can be obtained by breaking the symmetry of the nanoaperture. Moreover, the localized field enhancement at the two resonant peaks is larger than that of solitary BNAs. The phenomenon of large localized field enhancement can be explained by the double interaction between the composite structure and incident light. First, the incident light is coupled into ANAs. Then, the concentrated near fields in ANAs have been further enhanced by BNAs, which result in a large near-field enhancement for CBAs. The resonant peaks of CBAs have a red shift compared with that of BNAs due to the coupling between BNAs and ANAs.

In order to understand the influence of the ANAs on near-field distribution and to explore the origin of dual resonant peaks, we simulate the normalized near-field distribution for solitary BNAs and CBAs at several special wavelengths. Figure 3a shows the normalized near-field distribution of a solitary BNA at a resonant wavelength of 640 nm. As is well known, the E-fields are formed symmetrically near the gap region because of the rigorous symmetry of the solitary BNA. However, the near-field distribution of the proposed CBAs has three kinds of modes, which are shown in Fig. 3b–d. When the wavelength of incident light is far away from the resonant peaks, such as beyond 828 nm, the E-fields are distributed symmetrically in the gap region of the BNA. The CBAs can generate an asymmetric distribution, while the incident light is located at the two resonant peaks P_1 and P_2 . The E-field is mostly concentrated near one of the triangle tips. This kind of asymmetric distribution is attributed to the two distinct waveguide modes from the large and small rectangular

nanoapertures. The triangles of the BNA further collect the waveguide modes of the ANA resulting in the asymmetric distribution. Therefore, indirect manipulation of localized fields can be realized by ANAs while keeping BNAs fixed. The sensitivity and resolution of some applications, such as SERS and nanolithography, can be further improved by reducing the size of the localized field while maintaining a large localized field intensity. Meanwhile, dynamic shifting of the localized field distribution from one triangle to the other triangle can be employed to trap or sort nanoscopic matter [17, 18].

Influences of the Degree of Asymmetry

To demonstrate the influence of the degree of asymmetry on the optical properties of CBAs, we vary geometrical parameters of and extract some representative CBAs to show the shift of the resonant wavelength and the distribution of the localized field, as shown in Fig. 4. The normalized intensity spectra and localized field distributions for different parameters l_1 and l_2 are shown in Fig. 4. With the increasing of l_1 , the resonant peak P_1 has an obvious blue shift, but the resonant peak P_2 has only a slight shift. When the degree of asymmetry for CBAs is further reduced, only the resonant peak P_1 can be clearly seen in the normalized intensity spectra, which is in agreement with that of symmetric nanostructures. Meanwhile, when the degree of asymmetry is decreased, the normalized near-field distribution of CBAs becomes more and more uniform. This demonstrates that the dual resonant peaks and the asymmetric localized field distribution are completely induced by the ANAs. Figures 4e–h show the normalized intensity spectra and localized field distributions with varying of

Fig. 3 Calculated normalized near-field distribution at the resonant wavelength for **a** solitary BNAs at 640 nm, **b** CBAs at 828 nm, **c** CBAs at 700 nm, and **d** CBAs at 780 nm, where the cutting plane is in the middle of the BNAs in the x - y plane

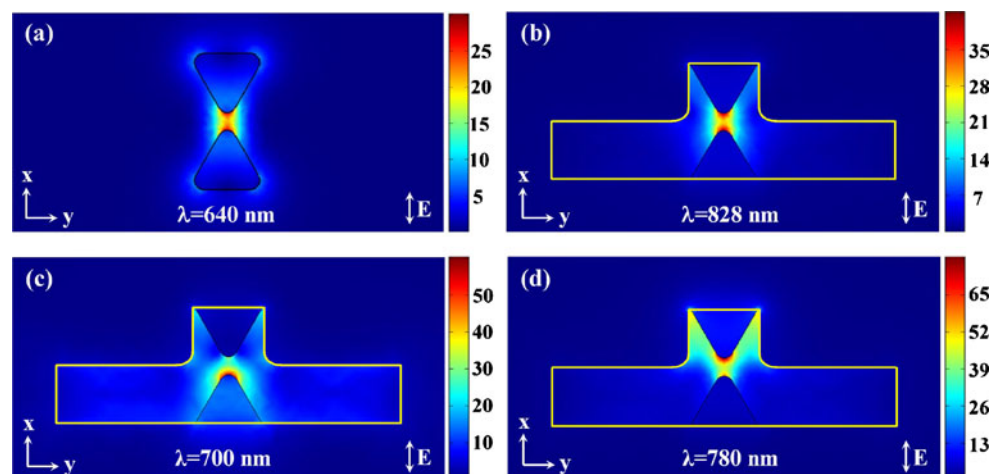
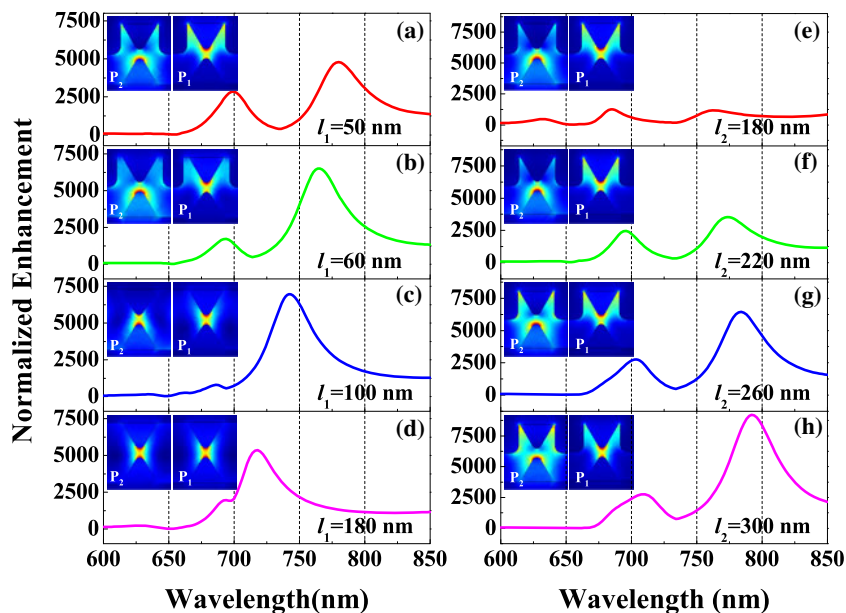


Fig. 4 Normalized intensity spectra and localized field distributions of the CBAs for different lengths of **a–d** the small rectangle, l_1 , and **e–h** the large rectangle, l_2 . *Insets* Normalized near-field distributions of the CBAs for the two resonant wavelengths in the gap region in the transverse x – y plane



the length of large rectangle l_2 . With increasing l_2 , the two resonant peaks of the CBAs exhibit an obvious red shift, and the localized field intensity is gradually increased. The parameter l_2 not only directly affects the high-energy mode P_2 but also indirectly influences the low-energy mode P_1 . This reveals that the two waveguide modes arise from some complex coupling effects between the two rectangles and not from just a simple superposition of the single waveguide modes for each rectangle. Essentially, the normalized near-field distributions of the CBAs maintain their asymmetry as the degree of asymmetry is further increased. Certainly, the length of the large rectangle should not exceed that of the small rectangle considerably; otherwise, the

interaction between the large rectangular nanoaperture and the incident light will become dominant.

In order to more clearly understand the tuning of the localized fields, we give the shift of the two resonant peaks as a function of the geometrical parameters l_1 and l_2 in Fig. 5. As mentioned before, the resonant peak P_1 has an obvious blue shift with the increasing of l_1 ; however, the two resonant peaks P_1 and P_2 exhibit an obvious red shift with the increasing l_2 . Therefore, flexible bidirectional adjustment can be realized by indirectly tuning l_1 and l_2 . This indirect method of adjustment allows a flexible manipulation of the nanoscale localized fields while maintaining the dimensions of the BNAs unchanged. In addition, there are more degrees of freedom to operate the resonant wavelengths and the localized field distributions than those of solitary BNAs. At the same time, it can still preserve the ability of nanoantennas to generate larger localized field enhancement than that of solitary BNAs. These advantages cannot be achieved by directly adjusting the dimensions of BNAs. Therefore, this kind of adjustment is important in practical applications for its convenience and ease of use.

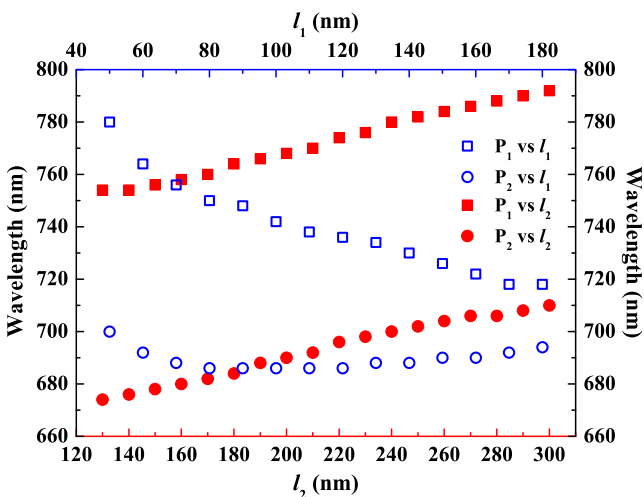


Fig. 5 Shift of the two resonant peaks P_1 (squares) and P_2 (circles) as a function of the geometrical parameters l_1 and l_2

Conclusions

In conclusion, we designed a novel asymmetric composite nanostructure CBAs consisting of BNAs and ANAs. The proposed CBAs cannot only produce a symmetric localized field distribution but also create two asymmetric localized field distributions in optical frequency.

We demonstrated that the two asymmetric modes arise from the two waveguide modes of the small and large rectangular nanoapertures. The resonant peaks of the CBAs can be easily tuned in both directions by indirectly adjusting the geometrical parameters of the ANAs, which obviously may improve the degree of freedom of operating the resonant wavelengths. Because of the controllability and tunability of the localized fields and the resonant wavelengths, CBAs are expected to be useful in a wide range of multicolor photodetection, optical filtering applications, super-resolution imaging, and optical trapping of nanoscopic matter.

Acknowledgements This work is supported by the Chinese National Key Basic Research Special Fund (No. 2011CB922003), the Natural Science Foundation of China (no. 61008002), the Specialized Research Fund for the Doctoral Program of Higher Education (no. 20100031120005), the Fundamental Research Funds for the Central Universities (nos. 65010801 and 65012351), and the 111 project (no. B07013).

References

- Lin T-R, Chang S-W, Chuang SL, Zhang Z, Schuck PJ (2010) Coating effect on optical resonance of plasmonic nanobowtie antenna. *Appl Phys Lett* 97:063106
- Chang Y, Wang S, Chung H, Tseng C, Chang S (2011) Large-area bowtie nanoantenna arrays fabricated with economic oxygen plasma-assisted nanosphere lithography. *Plasmonics* 6:599–604
- Hatab NA, Hsueh C-H, Gaddis AL, Retterer ST, Li J-H, Eres G, Zhang Z, Gu B (2010) Free-standing optical gold bowtie nanoantenna with variable gap size for enhanced Raman spectroscopy. *Nano Lett* 10:4952–4955
- Jiao X, Goeckeritz J, Blair S, Oldham M (2009) Localization of near-field resonances in bowtie antennae: influence of adhesion layers. *Plasmonics* 4:37–50
- Zhang Y, Dong X, Du J, Wei X, Shi L, Deng Q, Du C (2010) Nanolithography method by using localized surface plasmon mask generated with polydimethylsiloxane soft mold on thin metal film. *Opt Lett* 35:2143–2145
- Xie Z, Yu W, Wang T, Zhang H, Fu Y, Liu H, Li F, Lu Z, Sun Q (2011) Plasmonic nanolithography: a review. *Plasmonics* 6:565–580
- Kinkhabwala A, Yu ZF, Fan SH, Avlasevich Y, Mullen K, Moerner WE (2009) Large single-molecule fluorescence enhancements produced by a bowtie nanoantenna. *Nat Photonics* 3:654–657
- Liaw J, Tsai H, Huang C (2012) Size-dependent surface enhanced fluorescence of gold nanorod: enhancement of quenching. *Plasmonics* 4:231–239
- Banaee MG, Crozier KB (2010) Gold nanorings as substrates for surface-enhanced Raman scattering. *Opt Lett* 35:760–762
- Tao J, Lu Y, Chen J, Lu D, Chen C, Wang P, Ming H (2011) Polarization-dependent surface-enhanced Raman scattering via aligned gold nanorods in poly(vinyl alcohol) film. *Plasmonics* 6:785–789
- Fromm DP, Sundaramurthy A, Schuck PJ, Kino G, Moerner WE (2004) Gap-dependent optical coupling of single bowtie nanoantennas resonant in the visible. *Nano Lett* 4:957–961
- Yang Y-Y, Zhang Y-L, Jin F, Dong X-Z, Duan X-M, Zhao Z-S (2011) Steering the optical response with asymmetric bowtie 2-color controllers in the visible and near infrared range. *Opt Commun* 284:3474–3478
- Zhang Z, Weber-Bargioni A, Wu SW, Dhuey S, Cabrini S, Schuck PJ (2009) Manipulating nanoscale light fields with the asymmetric bowtie nano-colorsorter. *Nano Lett* 9:4505–4509
- Palik ED (1998) Handbook of optical constants of solids, 2nd edn. Academic, New York
- COMSOL (2008) Multiphysics 3.4 TM. <http://www.comsol.com>. Accessed 1 May 2012
- Ibrahim IA, Mivelle M, Grosjean T, Allegre JT, Burr GW, Baida FI (2010) Bowtie-shaped nanoaperture: a modal study. *Opt Lett* 35:2448–2450
- Roxworthy BJ, Ko KD, Kumar A, Fung KH, Chow EKC, Liu GL, Fang NX, Toussaint KC (2012) Application of plasmonic bowtie nanoantenna arrays for optical trapping, stacking, and sorting. *Nano Lett* 12:796–801
- Roxworthy BJ, Chow KC (2012) Plasmonic nanotweezers: strong influence of adhesion layer and nanostructure orientation on trapping performance. *Opt Express* 9:9591–9603